J MATER SCI 41 (2006) 1725–1731

# Fabrication of three dimensional polymeric scaffolds with spherical pores

JUNCHUAN ZHANG, HONG ZHANG, LINBO WU, JIANDONG DING*
*Key Laboratory of Molecular Engineering of Polymers, Department of Macromolecular Science, Fudan University, Shanghai 200433, People's Republic of China*
*E-mail: jdding1@fudan.edu.cn*

**Published online:** 17 February 2006

This paper reports polymeric scaffolds with spherical internal macropores and relatively large external dimension. Paraffin spheres with the diameter of several hundred microns were prepared by a suspension technique. Particulate leaching technique based on this kind of spherical porogens was combined with room-temperature compression molding technique to fabricate biodegradable poly(D,L-lactic-*co*-glycolic acid) (PLGA) porous scaffolds potentially for tissue engineering or *in situ* tissue induction. The scaffolds exhibited ordered macropores with good pore interconnectivity. The porosity ranged from 80 to 97% adjusted simply by varying porogen content. The foams with porosity around 90% have compressive modulus over 3 MPa and compressive strength over 0.2 MPa. As preliminary cell experiments with 3T3 fibroblasts cultured on the porous scaffolds indicate, the processing procedure of the scaffolds has not brought with problem in cytotoxicity. 

## 1. Introduction

In tissue engineering or *in situ* tissue induction, temporary scaffolds are necessary to repair or reconstruct tissues or organs [1–7]. Many processing methods have already been developed in preparation of porous scaffolds as tissue engineering implants. The present techniques include fiber bonding [8, 9], particulate leaching [2, 10–20], temperature-induced phase separation [21–26], gas foaming [27, 28], and three-dimensional printing [29, 30] etc. Especially, the particulate leaching technique has been widely utilized in the fabrication of porous supports for tissue engineering. The pore structure, pore size, and density can easily be modulated by controlling the properties and content of porogens.

Inorganic salt porogens have, in most of cases of particulate leaching, been used due to facile sourcing and easy leaching. Nevertheless, since the pore shape is cubic as determined by the crystal shape of salt particulates such as sodium chloride, the interconnectivity between pores is not well defined. In order to improve the tissue engineering foams, an ordered pore structure resulting from spherical porogens might be helpful. Gelatin spheres were first tried to prepare tissue engineering scaffolds with spherical macropores [15]. It is a good attempt, although the internal pores shown in the SEM images are not very regular and the reported polymer foams exhibit low porosities (up to around 70%). Paraffin was then introduced to prepare spherical-pore scaffolds by Langer and his colleagues [14]. With a modified approach by reverse replica technique, spherical paraffin microparticles were employed to prepare ordered pore structures successfully in the group of Ma [31, 32]. Their scaffolds exhibited well-controlled architecture and wonderful pore interconnectivity. The main procedures are described as follows: first, to stack densely paraffin spheres and compress the assembly to a certain degree; second, to cast polymer solution (PLLA in pyridine) into the stack drop by drop; and then, to evaporate the solvent; to repeat the casting and evaporating again and again; to leach the paraffin and obtain a porous PLLA scaffold. Due to the dropping technique in scaffold processing, it is, although not impossible, hard to obtain a scaffold with high polymer content or "relatively low" porosity such as 90% because polymer solution cannot easily penetrate the densely packed assembly. The resulting scaffolds were over porous (usually among 94 and 99%) [31, 32], and thus mechanical moduli were far less than one MPa although a crystalline polymer poly(L-lactic acid) (PLLA) was used as skeletal material. As is well known, scaffolds with porosity around 90% are most frequently used in tissue engineering. It is

*Author to whom all correspondence should be addressed.
0022-2461 
DOI: 10.1007/s10853-006-2873-7

thus nontrivial to improve the fabrication process to prepare polymeric scaffolds with ordered spherical pores and more appropriate porosities.

This paper reports spherical-pore scaffolds with a series of medium and high porosities (from 80 to 97%), and the compressive moduli of our scaffolds composed of non-crystalline biodegradable polyesters are desired to be enhanced over one MPa at porosity around 90%. Meanwhile, relatively thick scaffolds with complicated shape are useful for mimicking most of organs except skin. To meet the above requirements, the paraffin porogening technique should be combined with a suitable shaping or processing approach.

The fabrication of tissue engineering scaffolds is related to at least two levels of dimension, one is internal porogening, the other is external shaping. In previous work, we described a new processing method and examined the degradation behavior of poly(D,L-lactic-*co*-glycolic acid) (PLGA) scaffolds [33]. A combined flexible-rigid mould was also designed [33, 34]. Instead using a dropping procedure, the mixture of concentrated polymeric solution and inorganic salt particulates was compressed into a predesigned mould. By this method, complex PLGA porous scaffolds can be shaped rather well. This paper combines our room-temperature compression molding approach [33, 34] with paraffin porogening method of Ma *et al*. [31] to fabricate relatively large polyester scaffolds with interconnected spherical macropores and wide porosity range. The compressive moduli of the resulting three dimensional PLGA scaffolds with porosity around 90% can be over one MPa. Preliminary cell experiments have also been performed to evaluate whether or not the processing procedure will bring any cytotoxic problem to the scaffolding materials.

## 2. Materials and methods

### 2.1. Materials

Poly(D,L-lactic-*co*-glycolic acid) with 85:15 copolymer molar ratio (PLGA85/15) in a granular form was purchased from Purac Inc. (Netherlands). The number average molecular weight determined by gel permeation chromatography (GPC, Agilent 1100, Agilent Co., USA) in tetrahydrofuran at 35°C was $2.90 \times 10^5$ and the polydispersity was 1.90.

The paraffin was with 58–60°C congealing point. The gelatin was in the chemical grade. Other chemicals were analytical grades and were used without further purification.

### 2.2. Preparation of spherical porogens

Paraffin spheres were prepared by quenching the emulsion suspension in ice water. Briefly, 20 g paraffin and 1 g gelatin were added into 400 $cm^3$ deionized water. The mixture was then heated to approximately 80°C and was mechanically stirred at 300 rpm to form a well-dispersed suspension. After 2 h, the melted paraffin spheres were solidified by adding 300 $cm^3$ ice water to the stirred suspension and cooling the mixture additionally with an ice water bath. The suspension containing the paraffin spheres was filtrated and subsequently rinsed with deionized water for several times.

After vacuum dried, the spheres were sifted with standard sieves. The paraffin spheres with the desired sizes were collected and stored in a vacuum desiccator until use.

### 2.3. Scaffold fabrication

Porous scaffolds were fabricated using room-temperature compression molding & particulate leaching method originally used for the preparation of scaffolds with salt particulates as porogens. In brief, 1 g PLGA85/15 was first dissolved in 5 $cm^3$ acetone. Sieved spherical porogens were then added into the polymer solution to form a paste-like composite. The composite was pressed into a predesigned mould cavity with the size of 10 mm in diameter and 10 mm in height, and then kept under pressure for 4 h at ambient temperature. The sample was released from the mould and stored in a vacuum oven for 48 h to remove residual solvent. After solvent evaporation, paraffin spheres were leached out using Soxhlet extractor with *n*-pentane as the solvent for 24 h. The samples were carefully dried at room temperature in a vacuum oven before characterization.

The images of scaffolds were captured by a digital camera (DSC-S75, Sony Co., Japan). Slices were obtained by cutting the porous scaffolds *via* a sharp blade. The cross-sectioned samples were coated with gold prior to scanning electron microscopy (SEM, Philips 30XL, Netherlands) observation.

### 2.4. Porosity measurement

The porosity was calculated from the weight or mass, and the volume of each cylindrical sample [15]. From the values of mass and volume, the apparent density $\rho_F$ of the foam was calculated. The porosity was then determined by

$$\varphi_V = 1 - \frac{\rho_F}{\rho_P} \tag{1}$$

where $\rho_P$ is the density of the scaffolding bulk material. The relative density $\rho_F/\rho_P$ reads $1-\varphi_V$, and is thus related to porosity. Five specimens were measured. The statistical data are shown as mean plus standard deviation.

### 2.5. Mechanical testing

The compressive modulus and compressive strength of the porous scaffolds were measured at ambient temperature. The samples were tested in an Instron Model 5561 Materials Testing Machine (Instron Co., Canton, MA, USA). Cylindrical scaffolds of approximately 10 mm in diameter and 10 mm in height were compressed at a cross-head

speed of 0.1 mm/s. Five specimens were tested for each sample.

### 2.6. Cell culture and characterization

To evaluate the cytotoxicity of the fabricated scaffolds, the porous slices were seeded with NIH 3T3 fibroblasts (Shanghai Cell Bank of Chinese Academy of Science). Cylindrical porous scaffolds were cut into round slices with diameter of 10 mm and thickness of 2 mm. Prior to cell seeding, the round slices were prewetted by immersing into 70% ethanol for 2 h and exchanged by excess of phosphate buffered saline (PBS) solution. After PBS removal, 0.2 $cm^3$ of cell suspension ($1.5 \times 10^5$ cells/$cm^3$) was seeded by pipette onto each slice to let the cell suspension to fulfill the pores. The slices maintained in 24-well tissue culture plates and were incubated at 37°C under 5% $CO_2$ for 2 h. Then 1.3 $cm^3$ of culture medium was added to each well of the culture plate. The culture plate was incubated under the same condition described above. The culture medium consisted of HEPES-buffered DMEM (Dulbecco's Modified Eagles Medium, Gibco, US) supplemented with 100 U/$cm^3$ of penicillin (Sigma), 100 $\mu$g/$cm^3$ of streptomycin (Amresco, US) and 10% calf serum.

Scanning electron microscopy (SEM) was employed to observe the morphology of 3T3 fibroblasts cultured on the scaffolds. For cell-seeded scaffolds, samples were fixed in 1% glutaraldehyde for 12 h, dehydrated in a graded series of ethanol aqueous solutions with the concentrations of 40, 50, 60, 70, 80, 90 and 100% in time sequence each for 15 min. After dried, the samples were sputter-coated with gold. The SEM experiment was operated at 20 kV to image samples.

Viability and proliferation of the cells cultured on the scaffolds were determined by an MTT (3-(4,5-dimethylthiazol-2-yl)-2,5-diphenyltetrazolium bromide) assay. Briefly, 0.1 $cm^3$ of MTT solution (5 kg/$m^3$ in PBS) was added into each well of a culture plate with scaffold slices and then incubated. The culture medium was removed after 4 h. The intracellular formazan was solubilized by adding 0.5 $cm^3$ of dimethyl sulfoxide (DMSO) into each well, and the plate was mildly shaken for 10 min to ensure dissolution of the formazan. The dissolved formazan solution (0.1 $cm^3$ per well) was added into a 96-well plate, and optical density (OD) of the solubilized formazan was obtained in Multiskan MK3 microplate reader (Multiskan Co., Finland) with a 570 nm wave length. The final solution in the MTT test of cell-free scaffold slices but under the same "culture" condition was used as blank in OD measurements in the MTT tests of the cell-loaded samples. The MTT tests were repeated three times for each condition.

## 3. Results and discussion

### 3.1. Scaffold fabrication and morphology observation

Room-temperature compression molding and paraffin particulate leaching was combined to prepare porous scaffolds in this paper. To obtain spherical porogens, paraffin spheres were prepared by quenching the emulsion suspension in ice water. After dried and sieved, the paraffin spheres were ready for porous scaffolds fabrication.

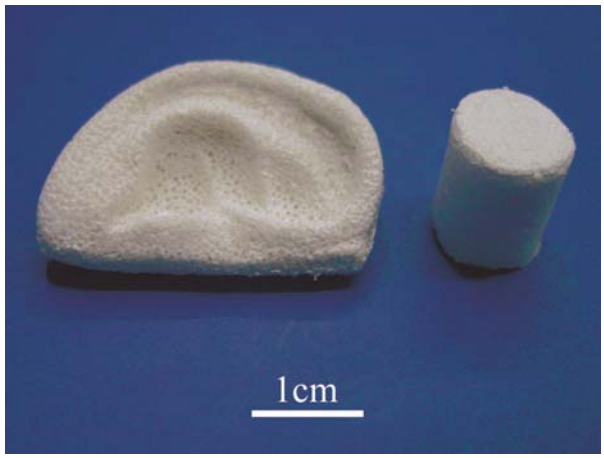


*Figure 1* Spherical-pore scaffolds with large dimension and complicated external shape fabricated via room-temperature compression molding and particulate leaching technique.

To eliminating the paraffin porogen after compression molding, the paraffin in the polymer-porogen composite was extracted by refluxed solvent continuously for 24 h. After being dried carefully, porous scaffolds were obtained. The resulting scaffolds are not sheet-like but relatively thick with large dimension and possibly with complicated shapes (Fig. 1). All of the following measurements were performed for the cylindrical scaffolds.

During the compression procedure, the paraffin spheres might deform and contact each other in tight connection. After eliminating the porogens, the global pores were left and the connecting apertures (CAs) were also generated. As illustrated in Fig. 2, the resulting PLGA85/15 porous scaffolds have a relatively ordered porous structure with well defined interconnectivity between the macropores. The connective holes between the pores would afford a pivotal tunnel for waste excretion and nutrition supply potentially for cell culture in potential tissue engineering.

The effect of particle content on the pore structure of PLGA porous scaffolds has also been examined. SEM images in Fig. 2 show the pore morphologies of PLGA85/15 cellular scaffolds associated with different porogen weight fractions of 75, 90 and 95%. Even at 75 wt% porogen content, the spherical cavity can connect to the adjacent ones through small connecting holes with tens of micron. With porogen weight content over 90 wt%, the CAs become as large as about one hundred microns, which might be sufficient for easy cell seeding and migration. The CA coverages in the images shown in Fig. 2 were further measured with the software of ImageJ 1.33u (Wayne Rasband, National Institutes of Health, USA). The results are 4, 20 and 24% associated with porogen contents of 75, 90 and 95%, respectively. Although the coverage just roughly indicates the interconnectivity, the

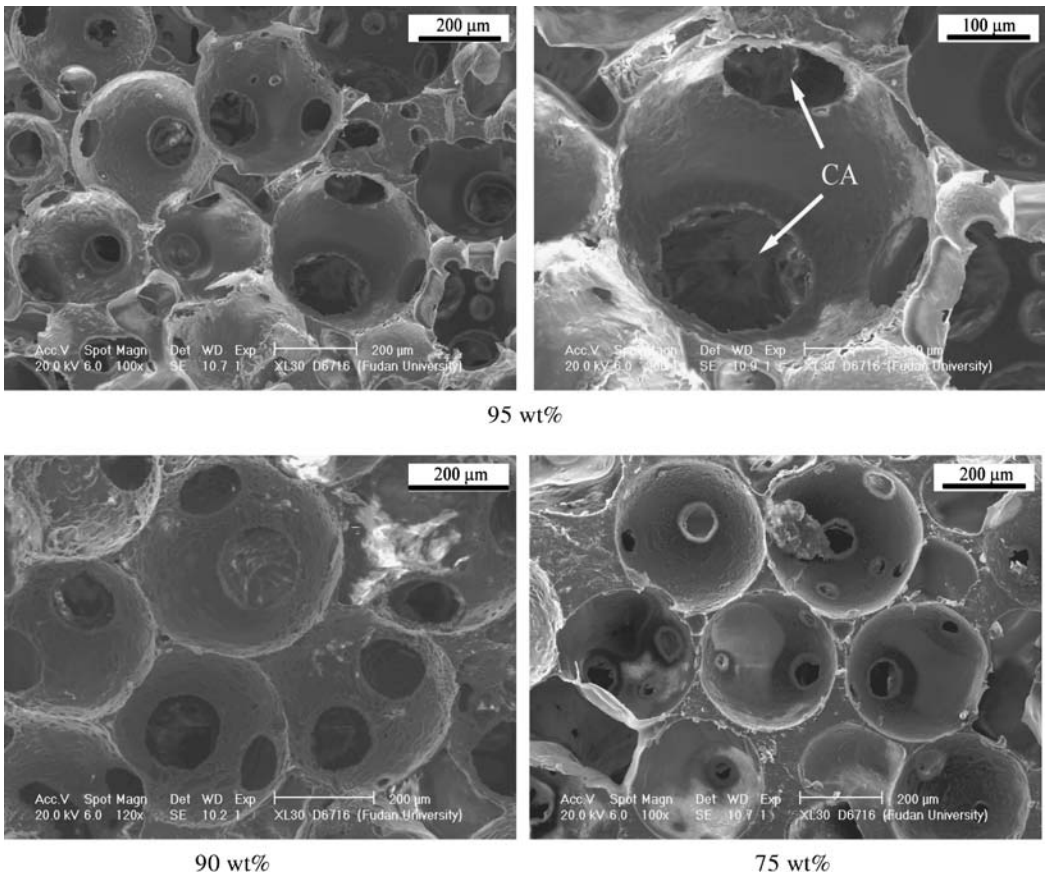


*Figure 2* SEM micrographs of spherical-pore PLGA85/15 scaffolds. The paraffin spheres were among 355–450 $\mu$m according to the sieves used. Marked under micrographs are weight fractions of porogen in fabrication. Two connective apertures (CAs) are specifically marked in the upper-right image. The two-dimensional coverage of the CAs with respect to the whole image plane is roughly calculated as 24% in the upper-left image, while those for the lower-left one and lower-right one are 20 and 4%, respectively.

calculation demonstrates that the interconnectivity of the macropores is enhanced at higher porogen content.

## 3.2. Scaffold porosity

In principle, if the density of polymer, $\rho_P$, and that of porogen, $\rho_S$, are known, the theoretical porosity of the underlying scaffolds with open-cell structure can be roughly estimated by Equation 2 [15].

$$\varphi_V\ (\%) = \frac{\varphi_W/\rho_S}{\varphi_W/\rho_S + (1-\varphi_W)/\rho_P} \times 100\% \qquad (2)$$

So, the porosity $\varphi_V$ is, although not equal to, strongly dependent of the weight content of porogen particles $\varphi_W$.

As illustrated in Fig. 3, the porosity increased with the weight fraction of the paraffin spheres and was dominated by the weight content of porogen particulate $\varphi_W$. The density of paraffin is approximately $0.90 \times 10^3$ kg/m$^3$, and that of PLGA85/15 is set as $1.29 \times 10^3$ kg/m$^3$ [8]. The theoretical line is based upon Equation 2, which is not a linear function but close to linear relation among the tested porosity range.

The experimental data is somewhat larger than the theoretical value at low content of particles, but close to the theoretical calculation at high content of paraffin spheres especially above 95 wt%. Small pores generated in solvent evaporation may contribute to porosity, as is well known. When the porogen fraction is low, the polymer fraction is usually high and more organic solvent is necessary to thoroughly solubilize the polymer, which leads to

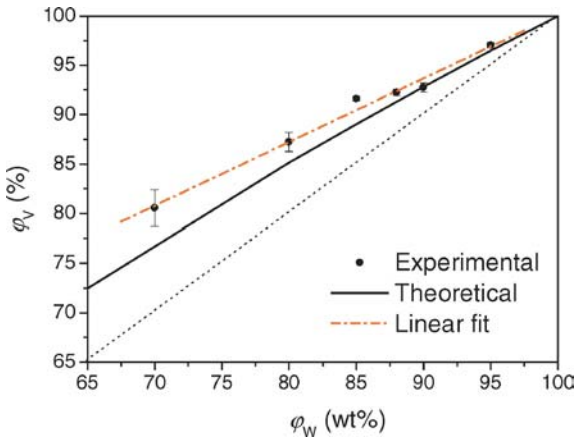


*Figure 3* Porosity of scaffold $\varphi_V$ versus weight fraction of paraffin porogen $\varphi_W$. Theoretical porosity line was calculated from Equation 2 and experimental data was measured with the mass and volume method according to Equation 1.

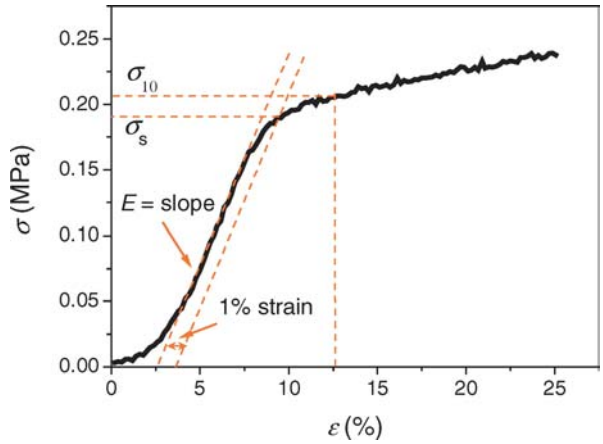


*Figure 4* A typical stress-strain curve of PLGA85/15 porous scaffold measured in our compression test. The scaffold resulted from 90 wt% porogen. Shown in the figure are presentations of compressive modulus $E$, compressive strength $\sigma_{10}$ and yielding strength $\sigma_S$ for a porous foam.

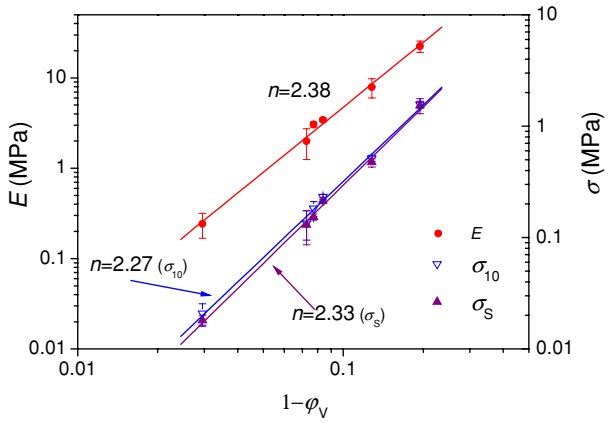


*Figure 5* Compressive modulus $E$, compressive strength $\sigma_{10}$ and yielding strength $\sigma_S$ of PLGA85/15 porous scaffolds as functions of relative density, $1-\varphi_V$. Foams were prepared with 355–450 $\mu$m spherical porogens.

more contribution of the solvent evaporation. The porosity could reach as high as 97% when 95 wt% porogen spheres were used in fabrication.

### 3.3. Mechanical properties

To be used as a supportive matrix, sufficient mechanical strength of the scaffold is essential for cell culture and ultimate organ formation. (The concrete values are dependent of the organs repaired. As usual, 100 kPa is necessary). A series of stress–strain curves of PLGA85/15 porous scaffold were obtained from our compression tests. A typical one is shown in Fig. 4. The compressive modulus $E$ was determined by the slope of the initial linear section of the stress-strain curve. The yielding strength $\sigma_S$ was defined as the intersection of the stress–strain curve with the modulus slope at an offset of 1% strain adopting the guidelines for compression testing of bone cement set in ASTM F451-99a. The compressive stress can also be measured as the stress at 10% strain ($\sigma_{10}$) according to ISO 844-2004 for determination of compression properties of rigid cellular plastics. In principle, the definition of $\sigma_S$ is only suitable for characterization of the compressive strength of a material such as PLGA exhibiting yielding behavior. This definition has been used in tissue engineering study by, for instance, Mikos and his colleagues [15]. Meanwhile, $\sigma_{10}$ is also a standard parameter in analysis of compressive test for a porous foam, and has been employed to characterize PLGA porous scaffolds [33]. Fig. 5 demonstrates that in the examined range, the two definitions of compressive stress do not lead to qualitative difference and thus are both justified to characterize compressive stress of tissue engineering scaffolds.

Compressive modulus and stress both decreased reasonably as the porosity increased. In all cases except at 97% porosity, the compressive modulus of the porous scaffolds can reach the order of magnitude of MPa. So the mechanical properties of our scaffolds are quite satisfactory even at high porosities especially in the range

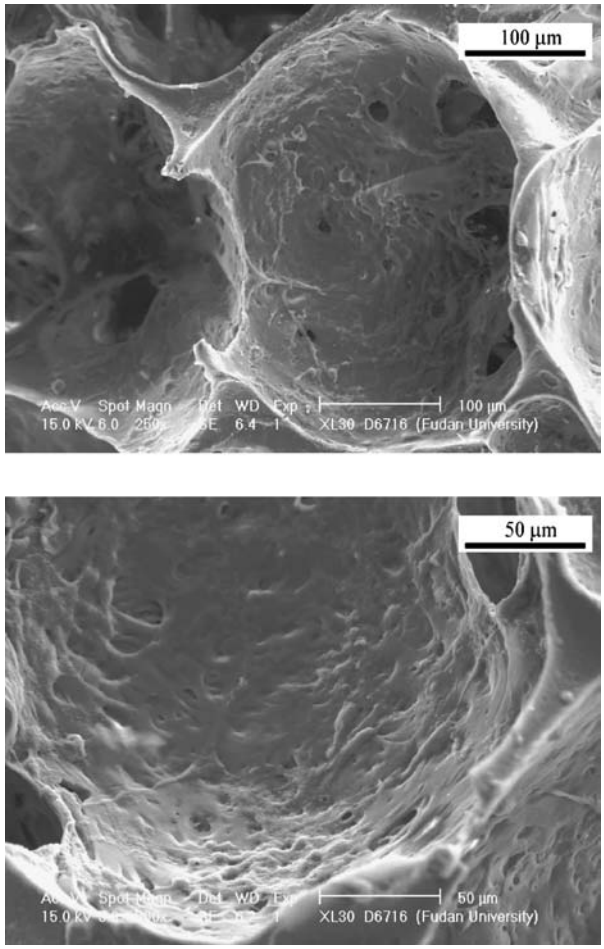


*Figure 6* SEM images of spherical-pore scaffold slices cultured with 3T3 fibroblasts after 48 h. The magnifications of the two images are ×250 and ×500, respectively.

between 90–95% which was believed the ideal void percent for cell culture in tissue engineering [35, 36].

For foams, there might be a power-law or scaling relationship as expressed in Equations 3 and 4

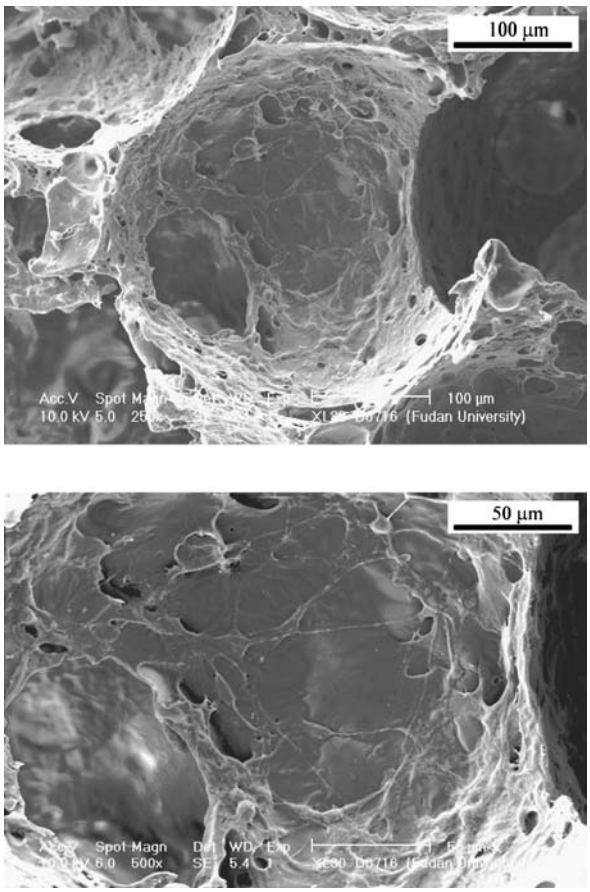


*Figure 7* SEM images of spherical-pore scaffold slices cultured with 3T3 fibroblasts after 72 h. The magnifications of the two images are ×250 and ×500, respectively.

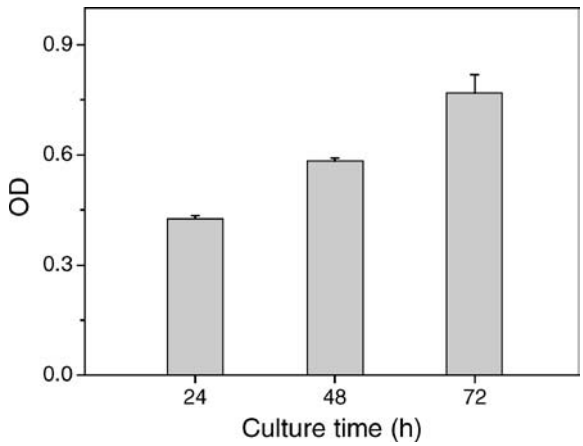


*Figure 8* MTT assay of 3T3 fibroblasts cultured on spherical-pore scaffolds.

[15, 18, 37–39]

$$E = C_1(1 - \varphi_V)^n \quad (3)$$

$$\sigma = C_2(1 - \varphi_V)^n \quad (4)$$

where $C$ and $n$ are constants. The scaling exponent is related to pore structure. For ideal foams with open pores made from materials which have a plastic yield point, the theoretical values of $n$ are 2 and 1.5 for predicting compressive modulus and yielding strength; for ideal honeycombs with polygonal pores, the above power law becomes 3 and 1 along transverse and axial loading, and 2 and 1 for predicting $\sigma$ under transverse and axial loading, respectively [15, 38].

The experimental results confirmed the scaling behavior of the mechanical properties with porosity. The fitted exponents (2.38, 2.33 and 2.27 for $E$, $\sigma_S$ and $\sigma_{10}$, respectively) are reasonably between 1 and 3. The linear fits also demonstrate that the scaling exponent for compressive modulus is basically similar to that of compressive strength. The detailed interpretation is still open so far.

### 3.4. Cytotoxicity evaluation

The fundamental requirement for a biodegradable polymer in medical application is its biocompatibility. Since PLGA has been approved by FDA as an implant biomaterial, we only need to confirm that the fabrication processing does not bring with cytotoxicity to the scaffolds.

Round discs were cut from thick cylindrical scaffolds, and fibroblasts were used to examine the effects of cell behaviors in the scaffolds obtained from our fabrication method. Figs 6 and 7 show SEM micrographs of the cells cultured for 48 and 72 h on the interior surfaces of the scaffolds, respectively. Cells cultured for 48 h adhered and spread on interior surfaces of the scaffolds. After cultured for 72 h, a large amount of extracellular matrix fibers were excreted by the cells spreading quite well on the internal pores in the scaffold.

To determine the cell proliferation on the spherical-pore slices quantitatively, viability of seeded cells on the scaffolds was tested by an MTT assay (Fig. 8), in which optical density reflecting total activity of an enzyme in cells is shown as a function of culture time of cells seeded on the surfaces of interior samples. An increase of OD indicates cell adhesion and proliferation in the scaffold. So, our fabrication method has not brought with cytotoxicity problem for the biomaterial. Moreover, cell viability implies that the transports of oxygen and nutrients in the scaffolds were rather efficient.

## 4. Conclusion

Combining room temperature compression molding and paraffin sphere leaching technique, the PLGA85/15 macropore scaffolds with spherical internal pores and relatively large external dimension have been fabricated. Porous scaffolds of various pore sizes and porosities (80 to 97%) were obtained. Ordered internal spherical macropores with good interconnectivity have been observed. The amorphous PLGA scaffolds exhibited rather good mechanical properties with compressive modulus over 3 MPa and compressive strength over 0.2 MPa even at high porosity around 90%. Cell evaluation experiments show that 3T3 fibroblasts not only adhered to the scaffolding materials but also started to spread with secretion of

extracellular matrix. The phenomena are intriguing due to the lack of any surface modification in the scaffolds fabrication procedure. The biodegradable polymeric scaffolds with ordered internal pores, large and complicated external dimension and good mechanical property at high porosities around 90% might be prospective in tissue engineering or *in situ* tissue induction applications.


## Acknowledgement

The authors are grateful for the financial support from NSF of China (No. 20221402, No. 20374015, No. 30271293, No. 20574013, No. 50533010), the Key Grant of Chinese Ministry of Education (No. 305004), the Award Foundation for Young Teachers from Ministry of Education, 973 project, 863 project (No. 2004AA215170), Science and Technology Developing Foundation of Shanghai.


## References


1. R. P. LANZA, R. LANGER and J. VACANTI, in "Principles of Tissue Engineering" (Academic Press, Orlando, 2000).
2. A. G. MIKOS, A. J. THORSEN, L. A. CZERWONKA, Y. BAO, R. LANGER, D. N. WINSLOW and J. P. VACANTI, *Polymer* **35** (1994) 1068.
3. D. W. HUTMACHER, *Biomaterials* **21** (2000) 2529.
4. C. M. AGRAWAL and R. B. RAY, *J. Biomed. Mater. Res.* **55** (2001) 141.
5. X. H. LIU and P. X. MA, *Ann. Biomed. Eng.* **32** (2004) 477.
6. T. M. FREYMAN, I. V. YANNAS and L. J. GIBSON, *Prog. Mater. Sci.* **46** (2001) 273.
7. A. P. PEGO, A. A. POOT, D. W. GRIJPMA and J. FEIJEN, *J. Cont. Rel.* **87** (2003) 69.
8. A. G. MIKOS, Y. BAO, L. G. CIMA, D. E. INGBER, J. P. VACANTI and R. LANGER, *J. Biomed. Mater. Res.* **27** (1993) 183.
9. D. T. MOONEY, C. L. MAZZONI, C. BREUER, K. MCNAMARA, D. HERN, J. P. VACANTI and R. LANGER, *Biomaterials* **17** (1996) 115.
10. A. G. MIKOS, G. SARAKINOS, S. M. LEITE, J. P. VACANTI and R. LANGER, *ibid.* **14** (1993) 323.
11. G. P. CHEN, T. USHIDA and T. TATEISHI, *ibid.* **22** (2001) 2563.
12. H. R. LIN, C. J. KUO, C. Y. YANG, S. Y. SHAW and Y. J. WU, *J. Biomed. Mater. Res.* **63** (2002) 271.
13. W. L. MURPHY, R. G. DENNIS, J. L. KILENY and D. J. MOONEY, *Tissue Eng.* **8** (2002) 43.
14. V. P. SHASTRI, I. MARTIN and R. LANGER, *Proc. Natl. Acad. Sci. USA* **97** (2000) 1970.
15. R. C. THOMSON, M. J. YASZEMSKI, J. M. POWERS and A. G. MIKOS, *J. Biomater. Sci.-Polym. Ed.* **7** (1995) 23.
16. R. Y. ZHANG and P. X. MA, *J. Biomed. Mater. Res.* **52** (2000) 430.
17. C. J. LIAO, C. F. CHEN, J. H. CHEN, S. F. CHIANG, Y. J. LIN and K. Y. CHANG, *ibid.* **59** (2002) 676.
18. Q. P. HOU, D. W. GRIJPMA, and J. FEIJEN, *Biomaterials* **24** (2003) 1937.
19. *Idem., J. Biomed. Mater. Res. Part B* **67B** (2003) 732.
20. S. H. OH, S. G. KANG, E. S. KIM, S. H. CHO and J. H. LEE, *Biomaterials* **24** (2003) 4011.
21. Y. S. NAM and T. G. PARK, *J. Biomed. Mater. Res.* **47** (1999) 8.
22. K. WHANG, C. H. THOMAS, K. E. HEALY and G. NUBER, *Polymer* **36** (1995) 837.
23. Z. W. MA, C. Y. GAO, Y. H. GONG and J. C. SHEN, *J. Biomed. Mater. Res. Part B* **67B** (2003) 610.
24. F. J. HUA, T. G. PARK and D. S. LEE, *Polymer* **44** (2003) 1911.
25. P. X. MA and R. Y. ZHANG, *J. Biomed. Mater. Res.* **46** (1999) 60.
26. F. YANG, R. MURUGAN, S. RAMAKRISHNA, X. WANG, Y. X. MA and S. WANG, *Biomaterials* **25** (2004) 1891.
27. L. D. HARRIS, B. S. KIM, and D. J. MOONEY, *J. Biomed. Mater. Res.* **42** (1998) 396.
28. Y. S. NAM, J. J. YOON and T. G. PARK, *ibid.* **53** (2000) 1.
29. C. X. F. LAM, X. M. MO, S. H. TEOH and D. W. HUTMACHER, *Mater. Sci. Eng. C-Biomimetic Supramol. Syst.* **20** (2002) 49.
30. G. CIARDELLI, V. CHIONO, C. CRISTALLINI, N. BARBANI, A. AHLUWALIA, G. VOZZI, A. PREVITI, G. TANTUSSI and P. GIUSTI, *J. Mater. Sci.-Mater. Med.* **15** (2004) 305.
31. P. X. MA and J. W. CHOI, *Tissue Eng.* **7** (2001) 23.
32. V. J. CHEN and P. X. MA, *Biomaterials* **25** (2004) 2065.
33. L. B. WU and J. D. DING, *ibid.* **25** (2004) 5821.
34. L. B. WU, H. ZHANG, J. C. ZHANG and J. D. DING, *Tissue Eng.* **11** (2005) 1105.
35. L. E. FREED, J. C. MARQUIS, A. NOHRIA, J. EMMANUAL, A. G. MIKOS and R. LANGER, *J. Biomed. Mater. Res.* **27** (1993) 11.
36. L. E. FREED, G. VUNJAKNOVAKOVIC, R. J. BIRON, D. B. EAGLES, D. C. LESNOY, S. K. BARLOW and R. LANGER, *Bio-Technology* **12** (1994) 689.
37. L. J. GIBSON and M. F. ASHBY, in "Cellular Solids: Structure and Properties" (Cambridge University Press, Cambridge, 1997).
38. I. ZEIN, D. W. HUTMACHER, K. C. TAN and S. H. TEOH, *Biomaterials* **23** (2002) 1169.
39. J. L. WILLETT and R. L. SHOGREN, *Polymer* **43** (2002) 5935.



*Received 12 March*
*and accepted 7 June 2005*